GPS Solutions (2024) 28:52
https://doi.org/10.1007/s10291-023-01593-4

ORIGINAL ARTICLE

Performance evaluation of real-time orbit determination for LUTAN-01B satellite using broadcast earth orientation parameters and multi-GNSS combination

Min Li[1,2] · Yubin Wang[1] · Wenwen Li[1,3] · Kecai Jiang[1] · Yu Zhang[1] · Haixia Lyu[1,4] · Qile Zhao[1,2]

Received: 27 March 2023 / Accepted: 29 November 2023 / Published online: 29 December 2023

Abstract
Real-time orbit determination (RTOD) for spacecraft using the space-borne GNSS technique needs earth orientation parameters (EOPs) for the required coordinate transformation between earth-fixed and inertial reference frames. GPS and BDS transmit EOPs in modernized navigation messages, which enables GNSS-equipped spacecraft to update EOPs onboard and improves the RTOD automaticity. However, the impact of broadcast EOP errors on RTOD has not yet been evaluated. With the GPS and BDS-3 observations collected from a Chinese low-earth orbit (LEO) mission, the LUTAN-01B satellite, we analyze the LEO RTOD performance with broadcast EOPs and GPS/BDS-3 combination for the first time. In RTOD, we parameterize the ephemeris signal-in-space range error (SISRE) to account for its slow-varying signature and to compensate for the EOP errors. Without estimating SISRE, the RTOD precision using broadcast EOPs is 70.1 cm with only GPS observations and 42.4 cm with only BDS-3, revealing degradations of 5.1 cm (7.8%) and 3.3 cm (8.4%) compared to those using the precise C04 EOPs, respectively. With SISRE estimated, the impact of broadcast EOP error is compensated and the RTOD precisions with broadcast EOPs show identical results to those with C04, reaching 36.3 cm with GPS and 25.8 cm with BDS-3. Combining GPS and BDS-3 further improves the RTOD precision to 23.9 cm. Furthermore, we show that the RTOD precision can be further improved by using GPS and BDS broadcast EOPs' differences to correct ephemeris rotation errors. With this correction, the precision improvement of BDS-3 independent and GPS/BDS-3 combined RTOD increases significantly when BDS-3 broadcast EOPs suffer large errors due to long update intervals. During the experiment period, their maximum orbital improvements reach 10.2 and 7.7 cm, respectively, while the average improvements are both around 1.5 cm.

Keywords Real-time orbit determination · GPS · BDS-3 · Broadcast EOP · Broadcast ephemeris · LUTAN-01B satellite

Introduction

The development of low-earth orbit (LEO) satellites requires high-precision and low-latency orbits. For instance, the LEO missions for earth radio occultation and altimetry need real-time orbit determination (RTOD) at a few centimeters for real-time atmosphere sounding and altimetry data processing (Desai and Haines 2003; Jayles et al. 2010; Tseng et al. 2018). The space-borne GNSS technique enables high-precision orbit determination (POD) due to its global coverage and precise observations. LEO orbit determination with space-borne GNSS can achieve centimeter-level accuracy, provided that precise GNSS orbit and clock products are used (Haines et al. 2004; Kang et al. 2006; Lemoine et al. 2010). However, the final precise GNSS products are only accessible by post-processing with delays of a few days, which cannot meet the timeliness requirement for

✉ Wenwen Li
cheeselee@whu.edu.cn

1 GNSS Research Center, Wuhan University, No. 129 Luoyu Road, Wuhan 430079, China

2 Hubei Luojia Laboratory, No. 129 Luoyu Road, Wuhan 430079, China

3 Department of Land Surveying and Geo-Informatics, The Hong Kong Polytechnic University, 11 Yuk Choi Road, Hung Hom, Kowloon, Hong Kong, China

4 Department of Physics and Mathematics, University of Alcalá, 28801 Alcalá de Henares, Madrid, Spain

the abovementioned applications. In addition, although the International GNSS Service (IGS) ultra-rapid and real-time products have low latency, transmitting them to LEO satellites in real time is difficult.

GNSS broadcast ephemeris can be received globally in real-time and is suitable for onboard RTOD. However, the broadcast ephemeris error remains a main challenge for RTOD, and it includes both orbit and clock offset errors and can be characterized by the signal-in-space range error (SISRE) (Montenbruck et al. 2018). The GPS SISRE is typically at a level of 0.7 m, whereas the two new emerging systems, BDS-3 and Galileo, present superior quality (Carlin et al. 2021; Zhang and Pan 2022). Attributed to stable atomic clocks and short update intervals, the Galileo SISRE has achieved a level better than 0.3 m, making it the best among all GNSS constellations (Wu et al. 2020). With the application of the inter-satellite link (ISL) technique and hydrogen atomic clock, the third generation of BDS (BDS-3) indicates orbit and clock offset precisions of 0.4 m and 1.8 ns for the MEO satellites, respectively, leading to a SISRE level of 0.5 m, which is only half of that of the second generation of BDS (BDS-2) (Shi et al. 2020; Chen et al. 2021). Utilizing Galileo and BDS-3 can significantly enhance the RTOD accuracy. With real onboard Galileo observations, the Sentinel-6A spacecraft reveals a three-dimensional (3D) accuracy of 0.10 m, which is 2–3 times better than GPS (Montenbruck et al. 2022). Li et al. (2022) validated that an orbit precision of 0.23 m is feasible using onboard BDS-3 observations recorded on the Chinese oceanic mission satellite HY2D. However, the limitation of HY2D's inability to simultaneously track GPS and BDS-3 signals hinders the investigation of the RTOD performance with combined GPS and BDS-3 observations.

It should be noted that the above studies are based on a reduced-dynamic RTOD approach rather than a kinematic approach as the latter is particularly sensitive to severe GNSS data quality deteriorations such as GNSS data outages (Montenbruck et al. 2005). In a typical reduced-dynamic RTOD procedure based on GNSS broadcast ephemerides, earth orientation parameters (EOPs) are needed to form the coordinate transformation matrix between the earth-centered earth-fixed (ECEF) reference frame and the earth-centered inertial (ECI) frame (Montenbruck and Ramos-Bosch 2008). The full set of EOPs is manifested as the motions of the Earth's spin axis relative to the celestial sphere (precession and nutation) and those on the Earth's crust (polar motion), as well as the differences between the universal time and coordinated universal time (UT1-UTC; or its time-derivative length-of-day change) (Petit and Luzum 2010; Dehant and Mathews 2015). Since precession and nutation can be well represented by analytical models, only polar motion terms and UT1-UTC, which explicitly refer to Earth rotation parameters (ERPs), are required in practical applications such as RTOD. Currently, most LEO missions acquire ERP data via regular ground upload which is restricted to upload station distribution and data upload frequency. Thus, the automaticity of onboard RTOD is reduced (Wang et al. 2015).

Fortunately, GPS and BDS-3 have been transmitting ERPs in modernized civil navigation (CNAV) messages worldwide, e.g., the GPS CNAV and CNAV-2 messages, as well as BDS CNAV-1, CNAV-2, and CNAV-3 messages (CSNO 2017a, 2017b; IS-GPS-200M 2021). In accordance to the GPS and BDS Interface Control Documents (ICDs), we use the term EOPs to describe these parameters, although they more strictly refer to the designation ERPs. These GNSS broadcast EOPs enable GNSS-equipped spacecraft to automatically update EOPs onboard, eliminating the requirement for external data. IGS has started to disseminate GNSS broadcast EOP data via navigation files in the latest receiver independent exchange (RINEX) 4.00 format since 2022 (Romero 2021). Steigenberger et al. (2022) evaluated the multi-GNSS broadcast EOP quality. The root-mean-square (RMS) errors of GPS broadcast EOPs are 0.96 mas for polar motion and 0.15 ms for UT1-UTC. In contrast, the RMS values of BDS-3 EOPs are 2.41 mas and 0.51 ms, respectively, which are more than twice those of GPS. With EOP errors of this magnitude, the orbit rotation error at the altitudes of LEO satellites can reach the centimeter or even decimeter level. Thus, it is necessary to investigate what precision the onboard RTOD can reach using broadcast EOPs.

Moreover, GNSS broadcast EOPs can potentially benefit the GNSS RTOD precision as they are found to be strongly coupled with the broadcast ephemeris rotation error. Due to errors in the EOPs adopted for broadcast ephemeris generation, the GNSS ephemeris suffers orientation deficiency, which is shown as a constellational rotation error. Among all GNSS systems, BDS indicates the most prominent rotation errors mainly at the non-radial components at a magnitude of 0.15 m due to its worst EOP precision (Chen et al. 2022). Li et al. (2023) revealed that such rotations can be represented by broadcast EOP errors. The correlation coefficients between the polar motion errors and *X*/*Y*-axis rotations exceed 0.88 and 0.77 for GPS and BDS, respectively, whereas there is little dependence of the *Z*-axis rotation on the UT1-UTC error. By correcting BDS-3 ephemeris rotation errors via EOP alignment, precise positioning based on GPS and BDS-3 ephemerides reveals a notable improvement in the north component by 21.9%. However, currently there are still no reports on improving LEO RTOD precision by considering ephemeris rotation correction using broadcast EOPs.

The LUTAN-01B (LT-01B) satellite is a Chinese LEO synthetic-aperture-radar (SAR) satellite for geological observation. It carries a suite of GNSS receivers and antennas that can track GPS and BDS-3 signals onboard. Using

the LT-01B onboard GNSS data, we for the first time investigate the RTOD performance with GPS/BDS-3 combination and analyze the impact of broadcast EOP errors on RTOD. Moreover, as a benefit of utilizing broadcast EOPs, the broadcast EOP alignment method for correcting ephemeris rotation errors is also validated for RTOD. Following the introduction section, a brief description of the LT-01B mission is presented. Then, the GPS and BDS-3 broadcast EOP precisions are evaluated. The LT-01B satellite RTOD is performed with different EOP datasets and using different constellations to analyze the impact of broadcast EOP errors. Then, the ephemeris rotation correction using broadcast EOPs is investigated for RTOD. Our conclusions are summarized in the last section.

Satellite platform

The LT-01 mission is an L-band SAR satellite mission developed by the China Centre for Resources Satellite Data and Application (CRESDA) for monitoring the geological environment, landslides, and earthquake disasters. The LT-01 constellation consists of two LEO satellites named LT-01A and LT-01B which were launched on January 26 and February 27, 2022, respectively. They are both in a sun-synchronous orbit with an altitude of 600 km and an inclination of 97.8°.

For onboard performance comparison and mutual backup, each of the LT-01 satellites is equipped with a pair of dual-constellation GNSS receivers that are capable of tracking both GPS and BDS multi-frequency signals. The onboard receivers track the L1 C/A and L2 $P(Y)$ signals for all GPS satellites. The legacy B1I and B3I signals are tracked for all BDS-2 and BDS-3 satellites excluding the geostationary earth orbit (GEO) satellites, whereas the new B1C and B2a signals are additionally tracked for BDS-3 satellites. Each receiver is connected to a separate antenna that is mounted on the top panel at an inclination of 30.5° degrees from the boresight direction. The antenna phase center offset (PCO) is described in the satellite body-fixed (SBF) frame defined as follows: the origin of the SBF frame is the center of mass; the $+Z$-axis points toward Earth center, the $+X$-axis points toward the satellite velocity direction, and the $+Y$-axis completes a right-hand coordinate system. The PCO vectors of the two antennas are $(-0.422, 1.828, -1.653)$ m and (0.418, 1.814, -1.620) m, respectively.

The LT-01B onboard GPS and BDS-3 observations from March 4th to April 9th, 2022, corresponding to the day of year (DOY) 63–99/2022, are collected for the RTOD analysis. The RINEX 4.00 version broadcast navigation file (referred to as BRD4 hereafter) is used in RTOD, which consists of both GNSS satellite ephemeris and broadcast EOP data. For comparison analysis, we utilize the post-processing high-precision C04 EOP product generated by International Earth Rotation and Reference Systems Service (IERS) as the reference value. It should also be noted that in this study we focus the investigation on the new BDS-3 signals, explicitly the B1C and B2a signals rather than the legacy B1I and B3I signals.

GPS and BDS-3 broadcast EOP evaluation

The broadcast EOPs are evaluated by comparison with IERS C04 EOP product. The IERS C04 product, generated from the combined EOP series of multiple space-geodetic techniques, demonstrates polar motion and UT1-UTC with high precisions of less than 0.05 mas and 0.01 ms, respectively (Bizouard et al. 2019). Due to the ambiguous specifications of subdaily tidal variations of the broadcast EOP data in GNSS ICDs, we emulate Steigenberger et al. (2022) to add subdaily corrections to C04 EOPs before performing the comparison.

The GPS and BDS EOP errors during DOY 63–99/2022 are shown in Fig. 1. They both exhibit significant periodical variations at diurnal and sub-diurnal frequencies, which should be attributed to the fact that the subdaily EOP variations cannot be fully represented through the linear fit function adopted by the GNSS broadcast EOPs. The GPS x_p and y_p errors fluctuate within ± 3.0 mas while the UT1-UTC errors are within ± 0.5 ms. Discontinuities are observed at midnight each day at a level of approximately 1.0 mas and 0.2 ms for polar motion and UT1-UTC, respectively, which should be attributed to the daily update of the GPS broadcast EOP prediction model (Steigenberger et al. 2022; Li et al. 2023). Compared to the GPS EOPs, the BDS EOP errors exhibit much larger variations, which are within ± 10.0 mas and approximately 0.6 ms for polar motions and UT1-UTC, respectively. There are six jump incidences in the BDS EOP error series with each spacing around 7 days. The discontinuities on DOY 70, 77, and 97 of 2022 even reach a level more than 9.0 mas for the polar motion and 0.4 ms for UT1-UTC. These jumps are presumably caused by the update of the BDS broadcast EOP prediction model. The overall RMS errors of GPS broadcast EOPs are 1.22 mas, 0.60 mas, and 0.12 ms for x_p and y_p, and UT1-UTC, respectively, while those of BDS EOPs are 4.01 mas, 1.91 mas, and 0.24 ms, respectively. The BDS polar motion errors are about three times those of GPS, while the BDS UT1-UTC errors about twice those of GPS.

Analysis of the EOP impact on RTOD

The strategy of LT-01B onboard RTOD with GPS and BDS-3 observations is presented. Then, we conduct RTOD with different EOP datasets to analyze its impact.

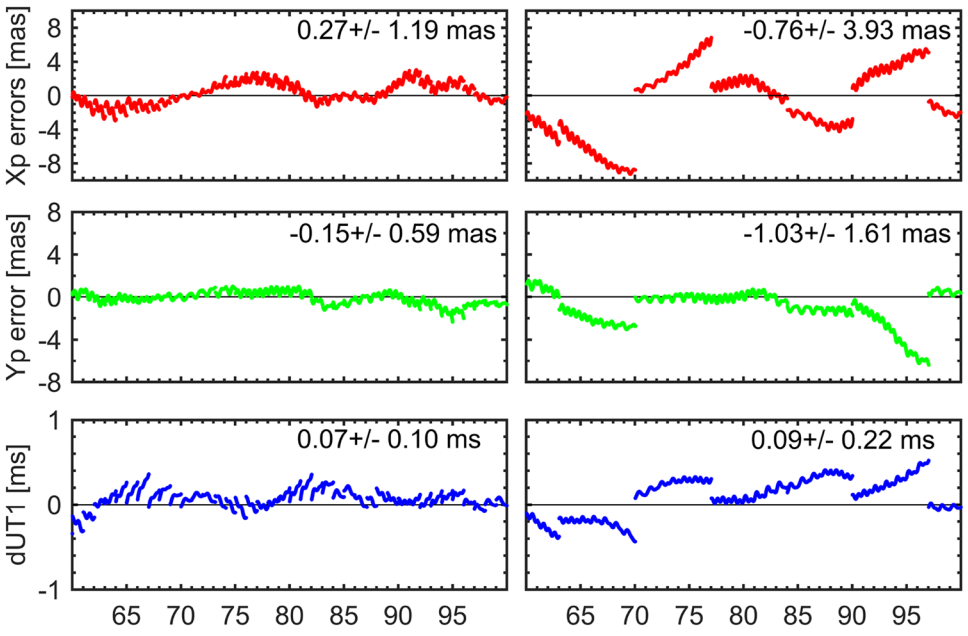

Fig. 1 GPS (left) and BDS (right) broadcast EOP errors compared to IERS C04 EOP product during DOY 63–99 in 2022 with an interval of 30 s. The corresponding mean and standard deviation values are given in the figure

Onboard RTOD strategy

The LT-01B onboard GPS and BDS-3 observations are processed with an RTOD software adapted from the post-precision GNSS data analysis software PANDA (Position and Navigation Data Analysis) developed at Wuhan University (Liu and Ge 2003). This software applies a typical reduced-dynamic orbit determination approach for RTOD (Montenbruck et al. 2005). It uses ionospheric-free (IF) code and carrier-phase observations as the basic observation model and implements the square root information filter (SRIF) to improve the numerical efficiency and stability. The detailed algorithm can be found in Li et al. (2022).

The dynamic models and observation models in LT-01B RTOD are presented in Table 1. Gravitational perturbations, including Earth gravity, tidal perturbations, N-body effects, and relativistic perturbations, are calculated using background models, e.g., EIGEN-06C (Shako et al. 2014) for non-spherical gravity and FES 2004 (Lyard et al. 2006) for oceanic tidal perturbations. Considering the efficiency requirement and memory limits for onboard RTOD, the EIGEN-06C is truncated to a degree and order of 50×50, whereas the ocean tide model is expanded up to a degree and order of 5×5. Non-gravitational perturbations such as the atmosphere drag and solar radiation pressure (SRP) are considered. The DTM 2013 model (Bruinsma 2015) is adopted to calculate the atmosphere mass density while a box-wing model based on LT-01B geometry is constructed for SRP. To compensate for the mis- and un-modeled perturbations, empirical accelerations in the along-track and cross-track directions are estimated as stochastic parameters at each epoch. The GPS legacy navigation message (LNAV) and BDS CNAV ephemerides are utilized for computing GPS and BDS-3 satellite orbits and clocks, respectively. Notably, the antenna phase center offsets of BDS-3 satellites are corrected to corresponding frequencies using the CSNO (China Satellite Navigation Office) antenna file. To compensate for the broadcast ephemeris ranging error, a separate SISRE parameter for each GNSS satellite is estimated as a random walk process considering its slow-varying signature (Gunning et al. 2019; Li et al. 2022). Considering the different precision levels of GPS and BDS-3 ephemerides, the process noise values of their SISRE parameters are set differently. The GPS and BDS broadcast EOPs are used for coordinate frame transformation in RTOD to evaluate the impact. In addition, RTOD with IERS C04 EOPs is also performed as the baseline solution for comparison.

With above RTOD strategies, the LT-01B orbits are estimated and then evaluated by comparison to the precise orbits derived from post-processing POD. The precision of LT-01B POD is at the 1.0 cm level as inferred from a typical 6-h orbit overlap comparison, which is sufficient for assessing the RTOD precision. For analysis of the RTOD convergence time, the convergence criterion is defined as the three-dimensional (3D) orbital error staying below 1.0 m for at least 10 min.

SISRE noise sensitivity on RTOD

Before performing LT-01B RTOD, the process noise of the SISRE parameter should be selected carefully to reasonably capture the slow-varying ephemeris ranging errors (Gunning et al. 2019). We test the process noise of the SISRE parameter with values from 0 to 10 mm,

Table 1 LT-01B RTOD strategy

Item	Description
Reference frame	
ECI reference frame	J2000.0
ECEF reference frame	GPS: the World Geodetic System 1984 (WGS84) (NGA 2021)
	BDS-3: BDS coordinate system (Han et al. 2021)
Precession and nutation	IERS-2010 (Petit and Luzum 2010)
EOP	IERS C04 (Bizouard et al. 2019) consistent with ITRF2014
	Broadcast EOPs (IS-GPS-200M 2021; CSNO 2017a, 2017b, 2020)
Dynamic model	
Gravity model	EIGEN-06C (Shako et al. 2014) truncated to a degree and order of 50×50
Solid earth tide	IERS Conventions 2010 (Petit and Luzum 2010)
Ocean tide model	FES 2004 (Lyard et al. 2006) truncated to a degree and order of 5×5
Relativity	IERS Conventions 2010 (Petit and Luzum 2010)
N-body perturbation	JPL DE405 (Standish and Williams 1992)
Solar radiation pressure	Box-wing model (Marshall and Luthcke 1994)
Atmosphere drag	DTM2013 (Bruinsma 2015); atmosphere drag coefficient estimated
Empirical acceleration	Sine and cosine accelerations in along-track and cross-track components
Observation model	
Observation interval	30 s
Observations	IF code and phase combination; (GPS: L1/L2; BDS-3: B1C/B2a)
Observation noise	IF code: 2.0 m; IF phase: 1.0 cm
Parameter a-prior accuracy and process noise ($\Delta t = 30$ s)	Position: 0.1 m and 0.2 m
	Velocity: 0.02 m/s and 0.2 m/s
	Drag coefficient: 10 and 0.001
	SRP coefficient: 10 and 0.001
	Empirical acceleration: 100.0 nm/s^2 and 0.05 nm/s^2
GNSS orbit and clock	GPS LNAV (IS-GPS-200M 2021) and BDS CNAV (CSNO 2017a, 2017b, 2020)
GNSS PCO	GPS: Ignored
	BDS-3: corrected from B3I to B1C and B2a PCOs according to CNSO antenna file
LT-01B PCO	Corrected using values provided by manufacture

of which the level of 0 mm indicates no SISRE estimation. The corresponding RTOD precisions are shown in Fig. 2. In the case of no SISRE estimation, the RTOD precision with BDS-3 observations reaches 39.1 cm, indicating an improvement of 39.8% compared to that with GPS (65.0 cm) since the BDS-3 ephemeris SISRE is only half that of GPS (Chen et al. 2021). Both the GPS and BDS RTOD achieve better precisions with the SISRE parameter estimated. The GPS-only RTOD accuracy decreases to approximately 40 cm when the SISRE noise is increased from 0 to 10 mm, and it achieves the best accuracy at 36.2 cm when the SISRE process noise is 5 mm. On the other hand, the BDS-only RTOD dramatically improves to 25.8 cm with a process noise of 1 mm. Continuously increasing the SISRE process noise degrades the RTOD precision. In summary, the best choice of the SISRE process noise is 5 mm for GPS and 1 mm for BDS-3. In the following RTOD calculations, the process noise of the

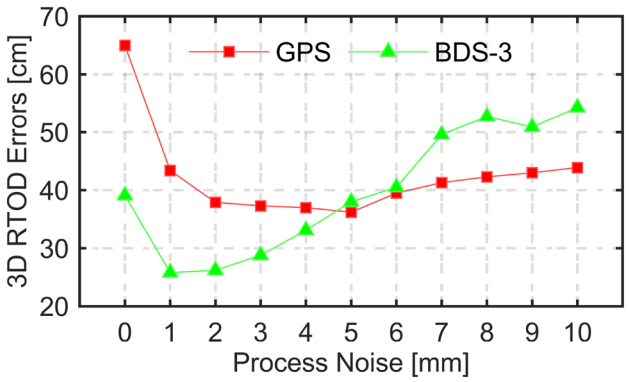

Fig. 2 GPS (red) and BDS-3 (green) independent RTOD errors under different process noise levels of SISRE parameters

SISRE parameter is set with this configuration if there is no specific notation.

RTOD with broadcast EOPs

To analyze the impact of broadcast EOPs on RTOD, we conduct LT-01B RTOD calculations using different constellations and different EOP datasets. Then, their RTOD precisions are assessed.

GPS/BDS-3 independent RTOD

We perform LT-01B RTOD using independent GPS and BDS-3 observations, during which different EOPs are employed, i.e., the C04 and broadcast EOPs. The RTOD calculation is not conducted on six separate days owing to data outages caused by satellite attitude maneuvers, i.e., DOY 68, 74, 85, 86, 92, and 98/2022. The RTOD filter is reinitialized at midnight each day to facilitate the convergence performance analysis.

The daily RTOD errors are calculated and shown in Fig. 3. For GPS RTOD with either C04 or broadcast EOPs, the along-track RMS values mainly vary within 0.2–0.4 m, while those at the cross-track and radial components at a smaller magnitude within 0.1–0.2 m. The BDS-3 RTOD presents a much better performance than GPS, revealing variations mainly within 0.1–0.2 m for all the three components. This is apparently attributed to the higher BDS-3 ephemeris precision than GPS. Both GPS and BDS-3 RTOD results show very few differences when using broadcast EOPs instead of C04 EOPs, indicating the broadcast EOP errors barely affect the RTOD precision. To further investigate this, we conduct RTOD again without estimating the SISRE parameters; the results are also shown in Fig. 3. When no SISRE estimated, both the GPS and BDS-3 RTOD precision manifest degradations of several decimeters while BDS-3 RTOD again shows an overwhelming performance than GPS. More significantly, the RTOD results using the broadcast EOPs show overall worse precisions than those using C04. For example, the BDS-3 RTOD deteriorates from 37.8 to 42.5 cm during DOY 95–97 when the BDS-3 y_p error vary around 6.0 mas and UT1-UTC errors about 0.4 ms.

The average RTOD precisions are calculated and listed in Table 2. When estimating no SISRE, the precisions of GPS-only RTOD with C04 EOPs are 56.4 cm, 22.2 cm, and 22.3 cm in the along-track, cross-track, and radial components, respectively, while those with GPS broadcast EOPs are 61.4 cm, 22.3 cm, and 24.2 cm, indicating a 3D orbital degradation of 5.1 cm (7.8%) due to broadcast EOP errors. For BDS-3, the orbit precisions obtained with C04 are 28.7 cm, 16.2 cm, and 21.7 cm, respectively, while those with BDS broadcast EOPs present degradations of 2.4 cm and 1.7 cm for the along-track and radial components. The 3D orbit precision shows degradations of 3.3 cm (8.4%) for BDS-3 RTOD. The RTOD errors caused by broadcast EOPs can be compensated well by SISRE parameters. With SISRE estimated, the along-track, cross-track, and radial precisions of GPS RTOD with either broadcast or C04 EOPs are improved to 30.5 cm, 13.7 cm, and 13.4 cm, respectively, whereas those of BDS-3 RTOD are 16.7 cm, 12.8 cm, and 14.4 cm, respectively. The BDS-3 RTOD shows a better performance than GPS by 10.5 cm (28.9%), primarily attributed to the superior BDS-3 ephemeris precision.

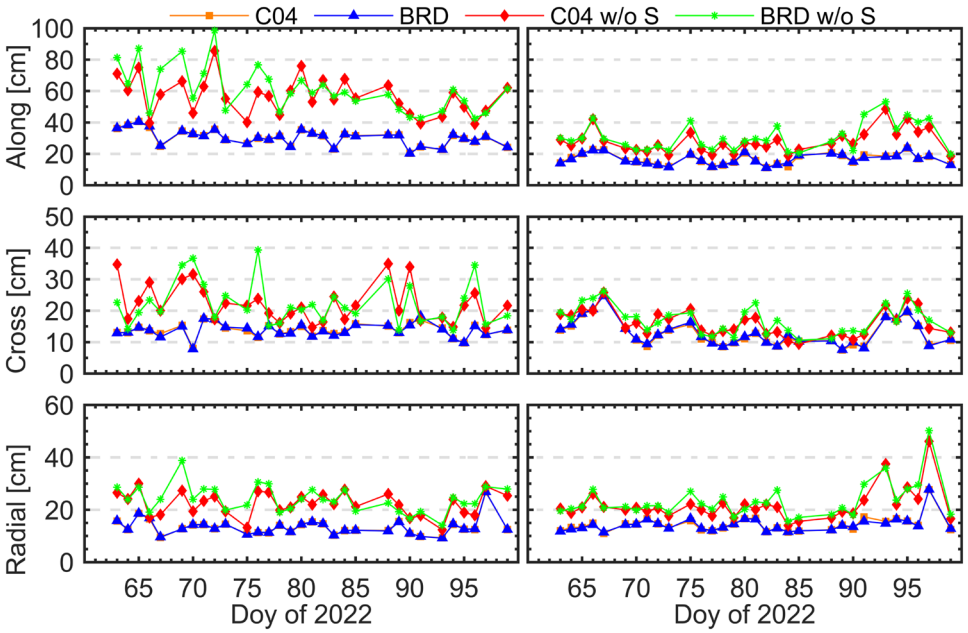

Fig. 3 Daily RMS errors of independent GPS (left panel) and BDS-3 (right panel) RTOD. The orange and blue dots and lines denote the RTOD results with SISRE estimation applied using the C04 EOPs (C04) and broadcast EOPs (BRD), respectively. The red and green dots and lines denote the RTOD results using C04 and broadcast EOPs but without estimating SISRE, respectively

Table 2 The RMS statistics of RTOD errors in the along-track, cross-track, radial, and 3D directions for GPS and BDS-3 RTOD applying C04 EOPs and broadcast EOPs

System	EOP	SISRE	Along-track (cm)	Cross-track (cm)	Radial (cm)	3D (cm)	Convergence (min)
GPS	C04	×	56.4	22.2	22.3	65.0	40.5
	C04	√	30.5	13.7	13.4	36.2	21.3
	GPS	×	61.4	22.3	24.2	70.1	45.7
	GPS	√	30.6	13.7	13.4	36.3	22.3
BDS-3	C04	×	28.7	16.2	21.7	39.1	16.7
	C04	√	16.7	12.8	14.4	25.8	16.3
	BDS	×	31.1	16.8	23.4	42.4	17.0
	BDS	√	16.6	13.0	14.3	25.8	16.5
GPS and BDS-3	C04	√	15.0	12.2	13.5	23.9	13.8
	BRD	√	15.2	12.3	13.5	24.1	13.9

Figure 4 shows the daily convergence time of each RTOD runs. The GPS-only RTOD converges mainly between 20 and 30 min while the BDS-3 RTOD mostly within 15–20 min. The convergence time for the entire arc is averaged for comparison, as shown in Table 2. With SISRE parameterization, the GPS RTOD shows an average convergence time of 21.3 min while BDS-3 RTOD performs much better, reaching 16.4 min. Note that both the GPS and BDS-3 RTOD results indicate that the utilization of broadcast EOPs barely affects the RTOD convergence time. Note the convergence time of BDS-3 RTOD is significantly better than the results obtained with HY2D by 23.0 min (Li et al. 2022), which is mainly attributed to the fact that LT-01B averagely tracks 3–4 more BDS-3 satellites than HY2D.

GPS/BDS-3 combined RTOD

Combining the GPS and BDS-3 observations increases the observation redundancy and improves the dilution of position (DOP), thus benefiting the combined RTOD precision. In Fig. 5, the frequency count of visible GPS/BDS satellites per epoch tracked by LT-01B is shown, while the position DOPs (PDOPs) with different constellations, such as GPS, BDS-3, and GPS and BDS-3 combination, are illustrated as well. Notably, only the satellite with a full presence of dual-frequency observations is considered since the IF carrier-phase and code combination model is used in RTOD. LT-01B can track more than four GPS and BDS-3 satellites for almost all epochs and the maximum satellite number reaches 12. The tracking performance for BDS-3 is slightly better than that for GPS. The proportion of epochs with a satellite number exceeding 9 is 29.8% for BDS-3, which is 11.2% higher than that for GPS. Statistically, the average satellite numbers for GPS and BDS-3 are 8.2 and 8.6, respectively; as a result, the average number of GPS and BDS-3 combinations reaches 16.8. Correspondingly, the GPS-only and BDS-only PDOP values vary mainly from 1.5 to 6.0, resulting in averages of 2.3 and 2.8, respectively. In contrast, the PDOP by the GPS and BDS-3 combination is significantly reduced between 1.0 and 2.0 with an average value of 1.4, indicating improvements of 39.1% and 50.0% against the GPS-only and BDS-only PDOP, respectively. In addition, frequent jumps are found in the GPS and BDS-3 PDOP series but are barely presented with the GPS and BDS-3 combination, indicating that the GPS and BDS-3 combination increases the PDOP stability as well.

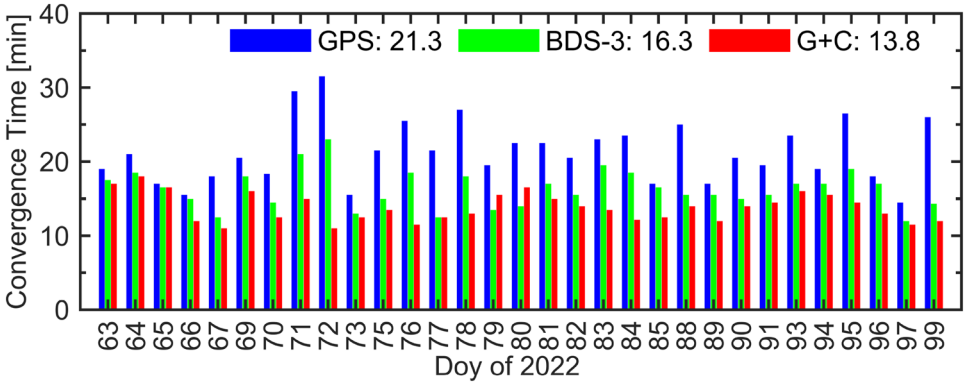

Fig. 4 Daily convergence time for GPS (blue), BDS-3 (red), and GPS and BDS-3 combined RTOD. The corresponding mean values are given in minutes

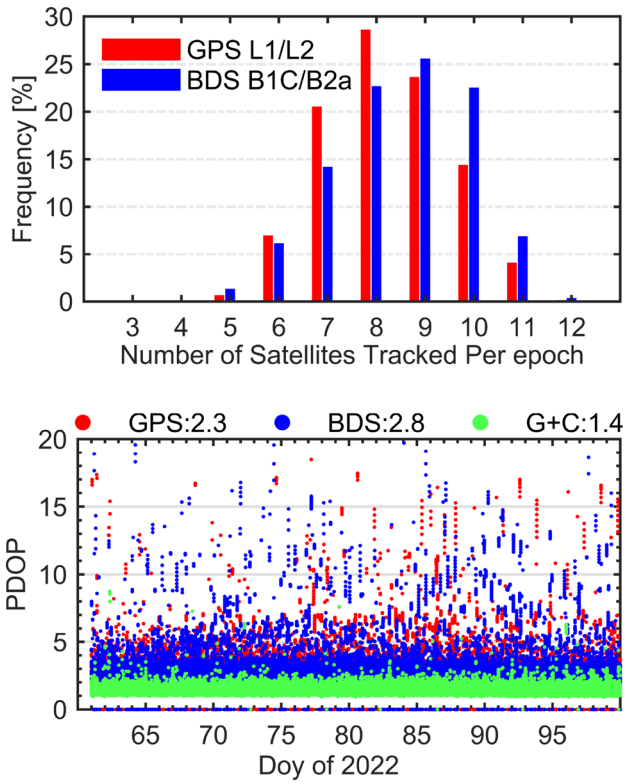

Fig. 5 Top: frequency count of the satellite number per epoch for GPS and BDS-3. Bottom: PDOP for GPS-only, BDS-3-only, and GPS and BDS-3 combined observations. The corresponding mean PDOP values are presented in the bottom panel

The average precision of the combined RTOD is shown in Table 2. The precisions with precise EOPs achieve 15.0, 12.2, and 13.5 cm at the along-track, cross-track, and radial components, respectively, while those with broadcast EOPs are at identical levels. The combined RTOD precision is much better than the GPS-only result with a significant 3D RMS reduction of 12.3 cm. However, the improvement over the BDS-3 independent RTOD is only 1.8 cm, indicating that the BDS-3 observations make the dominant contribution to the combined RTOD.

The combined RTOD presents a dramatic advantage in accelerating convergence speed comparing to single-system RTOD, which is primarily attributed to significant PDOP improvement with combined observations. As shown in Fig. 4, the daily convergence time of combined RTOD mainly varies between 10.0 and 20.0 min and the average value is 13.8 min, which is 7.5 and 2.5 min shorter than those of GPS and BDS-3 independent RTOD, respectively. This indicates improvements of 35.2% and 15.3%, respectively.

RTOD improvement with broadcast EOPs

The rotation errors in GNSS ephemerides present significant impacts on the ground positioning results even with SISRE parameterization (Li et al. 2023). Fortunately, they can be partly characterized by the broadcast EOP errors. In this section, we analyze the GPS and BDS-3 combined RTOD by considering ephemeris rotation correction with broadcast EOPs.

Rotation inconsistency correction for multi-GNSS ephemerides

The ephemeris rotation errors present prominent correlations with the broadcast EOP errors. Li et al. (2023) indicated that the polar motion x_p and y_p errors correspond to the *Y*/*X*-axis rotation errors, respectively. Therefore, the rotation correction for GPS and BDS-3 ephemerides can be denoted as,

$$r_{\mathrm{cor}} = r_{\mathrm{brd}} + \begin{bmatrix} 0 & R_z & -R_y \\ -R_z & 0 & R_x \\ R_y & -R_x & 0 \end{bmatrix} r_{\mathrm{brd}} \tag{1}$$

where r_{brd} and r_{cor} are the GNSS satellite position vectors calculated from broadcast ephemeris and those after rotation correction; and R_x, R_y, and R_z are the rotation parameters along the *X*-, *Y*-, and *Z*-axis, respectively. In particular, R_x and R_y exhibit strong correlations with the polar motion errors, specifically y_p and x_p, respectively. Thus, the rotation parameters can be linked to EOP errors as expressed below,

$$\begin{aligned} R_x &= y_{p,\mathrm{brd}} - y_{p,\mathrm{ref}} \\ R_y &= x_{p,\mathrm{brd}} - x_{p,\mathrm{ref}} \end{aligned} \tag{2}$$

where the polar motion with the subscripts brd and ref denotes the broadcast EOPs and reference EOPs, respectively. The C04 product is a good candidate for reference EOPs but is only available for post-analysis. For real-time applications such as RTOD, the GPS EOPs can be used instead. By referencing GPS broadcast EOPs, the BDS-3 ephemeris orientation is aligned to that of GPS. Notably, since there are few correlations between the R_z rotation and the UT1-UTC errors, we currently do not apply the R_z correction when using this EOP alignment approach.

RTOD improvement analysis

Considering the ephemeris rotation correction, BDS-3 RTOD and GPS/BDS-3 combined RTOD are performed with another two strategies; one uses C04 EOPs as references while the other uses GPS EOPs (denoted as ROT_4 and ROT_G, respectively). In order to get the best RTOD

performance by correcting all three axial rotation errors, RTOD is also performed by applying the orbital rotation parameters derived from the Helmert transformation between the broadcast ephemeris and the post-precise orbit products, denoted as ROT.

To illustrate the benefits of using ephemeris rotation correction, the RTOD errors in DOY 65–67/2022 are depicted in Fig. 6, during which the BDS-3 polar motion errors reach as large as 4.0–9.0 mas. The BDS-3 RTOD and combined RTOD reveal variations mainly within ± 1.0 m for each of the three components. With the ROT_4 and ROT_G strategies applied, both BDS-3 RTOD and combined RTOD present smaller along-track errors than those with no rotation correction; the reduction even reaches 0.5 m. This agrees with the BDS-3 polar motion errors during this period and indicates the RTOD calculations can benefit from ephemeris rotation correction using the broadcast EOPs.

To illustrate the RTOD precision improvement due to ephemeris rotation correction, the daily RTOD errors using the BRD, ROT_G, ROT_4, and ROT schemes are displayed in Fig. 7. Both BDS-3 and GPS/BDS-3 combined RTOD show RMS reductions of several centimeters in the

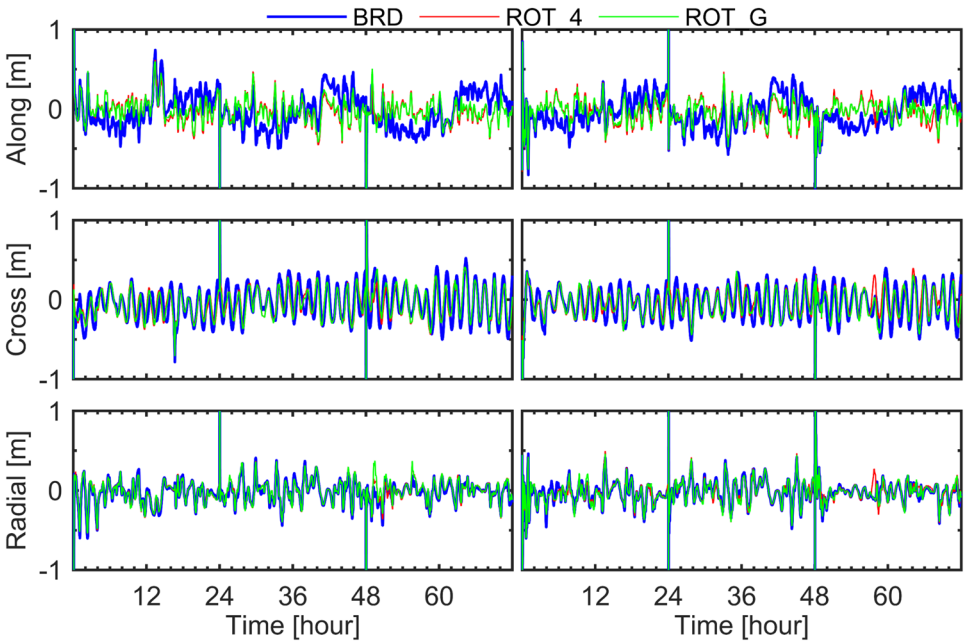

Fig. 6 Orbit errors of BDS-3 RTOD (left) and GPS and BDS-3 combined RTOD (right) during DOY 65–67/2022. All results are obtained using broadcast EOPs. The BRD result considers no ephemeris rotation correction. The spikes at daily boundaries are due to RTOD reinitializations at midnight each day

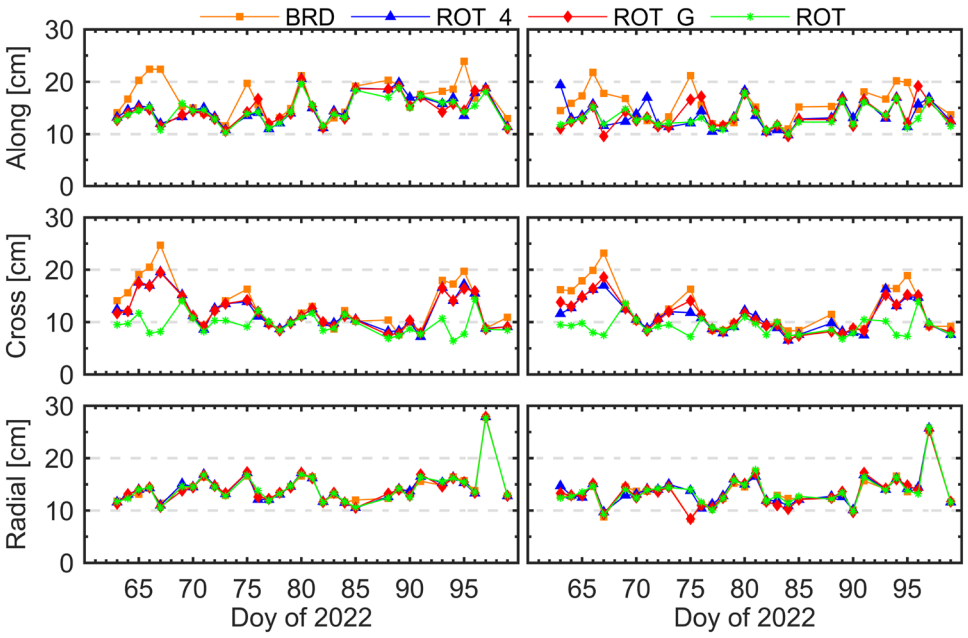

Fig. 7 Daily RMS values of BDS-3 RTOD (left) and GPS/BDS-3 combined RTOD (right) with different rotation correction strategies

along-track and cross-track components with ephemeris rotation corrected, and the reductions are more prominent when the update interval of BDS broadcast EOPs increases. For example, the BDS polar motion errors are as high as 6.0–9.0 mas during DOY 65–67/2022 and 93–95/2022 before the EOP update on DOY 70/2022 and 97/2022. In result, the along-track RMS error of the combined RTOD reaches 18.9 cm with the BRD strategy and is reduced to 13.7 and 13.3 cm with the ROT_G and ROT_4 strategies, respectively; meanwhile, the cross-track RMS also presents a decrease from 18.8 to 15.6 and 15.4 cm, respectively. By ephemeris correction via the broadcast EOP alignment method, the maximum 3D improvement reaches 10.2 cm for BDS-3 RTOD and 7.7 cm for GPS/BDS-3 combined RTOD. Moreover, comparison of the ROT results to ROT_4 and ROT_G reveals that a larger improvement for cross-track precision can be obtained by the additional *Z*-axis rotation correction. For instance, the average cross-track RMS of combined RTOD during DOY 65–67/2022 and 93–95/2022 is further improved to 8.4 cm with the ROT case, revealing reductions of 10.4, 7.2, and 7.0 cm against the BRD, ROT_G, and ROT_4 cases, respectively.

The average RMS errors for the ROT_G, ROT_4, and ROT schemes are listed in Table 3. The ROT_G and ROT_4 strategies arrive at very comparable precisions for both BDS-3 and GPS/BDS-3 combined RTOD, indicating that taking the GPS EOPs as references is sufficient for the EOP alignment approach. With these two schemes, the average along-track, cross-track, and radial precisions of the BDS-3 RTOD are 14.9, 12.0, and 14.4 cm, respectively, while those of the GPS/BDS-3 combined RTOD are 13.6, 11.0, and 13.7 cm, respectively. Their 3D precisions reach 24.3 cm and 22.5 cm, respectively, and indicate improvements of 1.5 and 1.6 cm against the RTOD results without rotation correction. The cross-track precisions of the BDS-3 RTOD and GPS/BDS-3 combined RTOD are further improved to 9.6 and 9.1 cm with the ROT scheme, respectively, mainly due to the *Z*-axis rotation correction. In result, their 3D precision improvements both increase to 3.0 cm. Since the *Z*-axis rotation error shows little dependence on the broadcast EOPs, an online estimation for it could be considered in onboard RTOD implementation.

Table 3 Precision statistics of BDS-3 and GPS/BDS-3 combined RTOD. Different ephemeris rotation correction strategies are applied for these RTOD solutions

System	Strategy	Along-track (cm)	Cross-track (cm)	Radial (cm)	3D (cm)
BDS-3	ROT_G	14.9	12.0	14.4	24.3
	ROT_4	14.8	12.0	14.3	24.1
	ROT	14.6	9.6	14.3	22.8
GPS and BDS-3	ROT_G	13.6	11.0	13.7	22.5
	ROT_4	13.5	11.2	13.4	22.4
	ROT	13.1	9.1	13.6	21.1

Conclusion

In this contribution, we investigate the RTOD performance using onboard GPS and BDS-3 data from a Chinese LEO mission LT-01B. Due to the advantage of real-time global availability, the broadcast EOPs from modernized GNSS navigation messages are applied in the LT-01B RTOD calculation, and their impact on RTOD is then analyzed.

The GPS and BDS-3 broadcast EOP quality are evaluated by comparison to the post-precise IERS C04 EOP product. The mean RMS errors of GPS x_p and y_p, and UT1-UTC, are 1.22 mas, 0.60 mas, and 0.12 ms, respectively, while those of BDS-3 are 4.01 mas, 1.91 mas, and 0.24 ms, respectively. BDS-3 broadcast EOPs are more than two times worse than GPS EOPs due to longer update intervals.

Considering the slow-varying SISRE of GNSS ephemeris, we estimate a SISRE parameter for each GNSS satellite as a random walk process during RTOD. Unintentionally, the SISRE parameterization approach compensates for both ephemeris errors and EOP errors. Without estimating the SISRE, the RTOD precision using broadcast EOPs is 70.1 cm for GPS-only RTOD and 42.4 cm for BDS-3 RTOD, indicating degradations of 5.1 cm (7.8%) and 3.3 cm (8.4%) compared to the results using precise EOPs. With the SISRE estimated, the 3D orbit precisions of GPS and BDS-3 independent RTOD with broadcast EOPs reach 38.1 and 25.8 cm, respectively, which are in the same magnitudes as those with C04 EOPs. Combining GPS and BDS-3 observations for RTOD further improves the orbit precision to 24.1 cm. Meanwhile, the combined RTOD shows a convergence time of 13.8 min, which is 35.2% and 15.3% faster than that of GPS and BDS-3 independent RTOD, respectively.

With the broadcast EOPs being able to represent ephemeris rotation errors, we further investigate the broadcast EOP alignment approach to improve the BDS-3 and GPS/BDS-3 combined RTOD. After applying this EOP alignment correction, the RTOD calculations show significant along-track and cross-track precision improvements, especially when BDS-3 broadcast EOPs suffer large errors due to long update intervals. The maximum 3D improvements of BDS-3 independent and GPS/BDS-3 combined RTOD reach 10.2 and 7.7 cm during the experiment period, while the average improvements are both around 1.5 cm.

To conclude, broadcast EOPs barely affect GPS and BDS-3 RTOD precision when the SISRE parameters are estimated. Moreover, the RTOD precision can be further improved if both GPS and BDS broadcast EOPs are available

as they can be used to correct the broadcast ephemeris rotation errors. Therefore, it is viable to use the EOP data from GNSS navigation messages for onboard RTOD calculation, which is advantageous in updating EOPs in real time and improving the automaticity of RTOD.

Acknowledgements Thank IGS and IERS for providing GNSS broadcast ephemeris and C04 EOP datasets. This study is sponsored by the National Natural Science Foundation of China (Grant Numbers 42004020, 42074032, 42204020, and 42030109), China Postdoctoral Science Foundation (Grant Numbers 2021M692460 and 2021M702507), and the Hong Kong Scholars Program. Haixia Lyu thanks University of Alcalá for the 2023-24 Giner de los Ríos Programme Grant.

Author contributions ML and WL conceptualized the idea; YW and WL analyzed the data and wrote the original draft; KJ and YW developed the software; ML and HL designed the experiment; QZ and YZ collected the data. All authors reviewed the manuscript.

Data availability The broadcast ephemeris files in RINEX 4.00 version can be publicly accessed from IGS data center. The IERS C04 EOP product is available at IERS data center. The onboard GNSS observations are available from the corresponding author upon request.

Declarations

Conflict of interest The authors declare no conflict of interest.

References

Bizouard C, Lambert S, Gattano C, Becker O, Richard J (2019) The IERS EOP 14C04 solution for Earth orientation parameters consistent with ITRF 2014. J Geod 93(5):621–633. https://doi.org/10.1007/s00190-018-1186-3

Bruinsma S (2015) The DTM-2013 thermosphere model. J Space Weather Space Clim 5:1–8

Carlin L, Hauschild A, Montenbruck O (2021) Precise point positioning with GPS and Galileo broadcast ephemerides. GPS Solut 25(2):77. https://doi.org/10.1007/s10291-021-01111-4

Chen G, Zhou R, Hu Z, Lv Y, Wei N, Zhao Q (2021) Statistical characterization of the signal-in-space errors of the BDS: a comparison between BDS-2 and BDS-3. GPS Solut 25(3):112. https://doi.org/10.1007/s10291-021-01150-x

Chen G, Wei N, Li M, Zhao Q, Zhang J (2022) BDS-3 and GPS/Galileo integrated PPP using broadcast ephemerides. GPS Solut 26(4):129. https://doi.org/10.1007/s10291-022-01311-6

CSNO (2017a) BeiDou navigation satellite system signal in space interface control document open service signal B1C (Version 1.0), December, 2017. http://www.beidou.gov.cn/xt/gfxz/201712/P020171226741342013031.pdf

CSNO (2017b) BeiDou navigation satellite system signal in space interface control document open service signal B2a (Version 1.0), December, 2017. http://www.beidou.gov.cn/xt/gfxz/201712/P020171226742357364174.pdf

CSNO (2020) BeiDou Navigation Satellite System Signal In Space Interface Control Document Open Service Signal B2b (Version 1.0). http://www.beidou.gov.cn/xt/gfxz/202008/P020200803362059116442.pdf. Accessed July 2020

Dehant V, Mathews PM (2015) Precession, nutation and wobble of the Earth. Cambridge University Press, Cambridge

Desai SD, Haines BJ (2003) Near-real-time GPS-based orbit determination and sea surface height observations from the Jason-1 mission special issue: Jason-1 calibration/validation. Mar Geod 26(3–4):383–397. https://doi.org/10.1080/714044528

Gunning K, Blanch J, Walter T (2019) SBAS corrections for PPP integrity with solution separation. In: Proceedings of ION ITM 2019, Reston, VA, USA 2019. https://doi.org/10.33012/2019.16739

Haines B, Bar-sever Y, Bertiger W, Shailen D, Pascal W (2004) One-centimeter orbit determination for Jason-1: new GPS-based strategies. Mar Geod 27(1–2):299–318. https://doi.org/10.1080/01490410490465300

Han C, Liu L, Cai Z, Lin Y (2021) The space–time references of BeiDou navigation satellite system. Satell Navig 2(1):1–10. https://doi.org/10.1186/s43020-021-00044-0

Jayles C, Chauveau JP, Rozo F (2010) DORIS/Jason-2: better than 10cm onboard orbits available for near-real-time altimetry. Adv Space Res 46(12):1497–1512. https://doi.org/10.1016/j.asr.2010.04.030

Kang Z, Tapley B, Bettadpur S, Ries J, Nagel P, Pastor R (2006) Precise orbit determination for the GRACE mission using only GPS data. J Geod 80(6):322–331. https://doi.org/10.1007/s00190-006-0073-5

Lemoine FG et al (2010) Towards development of a consistent orbit series for TOPEX, Jason-1, and Jason-2. Adv Space Res 46(12):1513–1540. https://doi.org/10.1016/j.asr.2010.05.007

Li M, Qin G, Jiang K, Wang Y, Zhao Q (2022) Performance assessment of real-time orbit determination for the Haiyang-2D using onboard BDS-3/GPS observations. Adv Space Res. https://doi.org/10.1016/j.asr.2022.09.050

Li W, Chen G, Li M, Wei N, Wang Y, Zhao Q (2023) Evaluation of GPS and BDS-3 broadcast earth rotation parameters: a contribution to the ephemeris rotation error. GPS Solut 27(3):115. https://doi.org/10.1007/s10291-023-01458-w

Liu J, Ge M (2003) PANDA software and its preliminary result of positioning and orbit determination. Wuhan Univ J Nat Sci 8(2):603–609. https://doi.org/10.1007/BF02899825

Lyard F, Lefevre F, Letellier T, Francis O (2006) Modelling the global ocean tides: modern insights from FES2004. Ocean Dyn 56(5):394–415. https://doi.org/10.1007/s10236-006-0086-x

Marshall JA, Luthcke SB (1994) Modeling radiation forces acting on TOPEX/Poseidon for precision orbit determination. J Spacecr Rockets 31(1):99–105. https://doi.org/10.2514/3.26408

Montenbruck O, Ramos-Bosch P (2008) Precision real-time navigation of LEO satellites using global positioning system measurements. GPS Solut 12(3):187–198. https://doi.org/10.1007/s10291-007-0080-x

Montenbruck O, van Helleputte T, Kroes R, Gill E (2005) Reduced dynamic orbit determination using GPS code and carrier measurements. Aerosp Sci Technol 9(3):261–271. https://doi.org/10.1016/j.ast.2005.01.003

Montenbruck O, Steigenberger P, Hauschild A (2018) Multi-GNSS signal-in-space range error assessment—methodology and results. Adv Space Res 61(12):3020–3038. https://doi.org/10.1016/j.asr.2018.03.041

Montenbruck O, Kunzi F, Hauschild A (2022) Performance assessment of GNSS-based real-time navigation for the Sentinel-6 spacecraft. GPS Solut 26(1):12. https://doi.org/10.1007/s10291-021-01198-9

NGA (National Geospatial-Intelligence Agency) (2021) (U) Recent update to WGS 84 reference frame and NGA transition to IGS ANTEX. https://earth-info.nga.mil/php/download.php?file=(U)WGS%2084(G2139).pdf

Petit G, Luzum B (2010) IERS conventions. IERS Technical Note No. 36

Romero I (2021) The receiver independent exchange format version 4.00. https://files.igs.org/pub/data/format/rinex_4.00.pdf

SAIC (2021) Interface specification IS-GPS-200: navstar GPS space segment/navigation user segment interfaces. https://www.gps.gov/technical/icwg/IS-GPS-200M.pdf

Shako R, Förste C, Abrikosov O, Bruinsma S, Marty J, Lemoine J, Flechtner F, Neumayer H, Dahle C (2014) EIGEN-6C: a high-resolution global gravity combination model including GOCE data. In: Flechtner F, Sneeuw N, Schuh W (eds) Observation of the system earth from space—CHAMP, GRACE, GOCE and future missions: GEOTECHNOLOGIEN science report No. 20. Springer, Berlin, Heidelberg, pp 155–161

Shi J, Ouyang C, Huang Y, Peng W (2020) Assessment of BDS-3 global positioning service: ephemeris, SPP, PPP, RTK, and new signal. GPS Solut 24(3):81. https://doi.org/10.1007/s10291-020-00995-y

Standish EM, Williams JG (1992) Orbital ephemerides of the Sun, Moon, and planets. In: Explanatory supplement to the astronomical, pp 279–323

Steigenberger P, Montenbruck O, Bradke M, Ramatschi M, Hessels U (2022) Evaluation of earth rotation parameters from modernized GNSS navigation messages. GPS Solut 26(2):50. https://doi.org/10.1007/s10291-022-01232-4

Tseng T, Chen S, Chen K, Huang C, Yeh W (2018) Determination of near real-time GNSS satellite clocks for the FORMOSAT-7/COSMIC-2 satellite mission. GPS Solut 22(2):47. https://doi.org/10.1007/s10291-018-0714-1

Wang F, Gong X, Sang J, Zhang X (2015) A novel method for precise onboard real-time orbit determination with a standalone GPS receiver. Sensors 15(12):30403–30418. https://doi.org/10.3390/s151229805

Wu W, Guo F, Zheng J (2020) Analysis of Galileo signal-in-space range error and positioning performance during 2015–2018. Satell Navig 1:6. https://doi.org/10.1186/s43020-019-0005-1

Zhang Z, Pan L (2022) Current performance of open position service with almost fully deployed multi-GNSS constellations: GPS, GLONASS, Galileo, BDS-2, and BDS-3. Adv Space Res 69(5):1994–2019. https://doi.org/10.1016/j.asr.2021.12.002

Min Li received his Ph.D. degree from Wuhan University in 2011. He is currently a professor at the GNSS Research Center of Wuhan University. His main work focuses on GNSS satellite orbit determination and precise point positioning as well as multi-GNSS processing using GPS, GLONASS, BeiDou, and Galileo.

Yubin Wang is a postgraduate student at the GNSS Research Center of Wuhan University. He obtained his bachelor's degree from Wuhan University in 2021. His current research mainly focuses on real-time and post-precise orbit determination of low-earth orbit satellites.

Wenwen Li obtained his doctoral degree at Wuhan University in 2019, and is a post-doctoral fellow at Wuhan University and the Hong Kong Polytechnic University. His main research interests include LEO/HEO satellite onboard GNSS data analysis, orbit determination, as well as applications in atmospheric sensing.

Kecai Jiang is currently a research assistant at the GNSS Research Center of Wuhan University. He received a Ph.D. at Wuhan University in 2020. His current research mainly focuses on LEO and side lobe signal HEO orbit determination using GNSS.

Yu Zhang is a doctoral postgraduate student at the GNSS Research Center of Wuhan University. He obtained his Master's degree from the Shanghai Astronomical Observatory in 2020. His current research mainly focuses on precise orbit determination of low-earth orbit formation satellites.

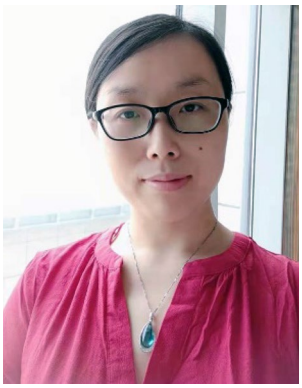

Haixia Lyu received her Bachelor's degree in 2010, Master's degree in 2012, both from Wuhan University; she obtained her doctoral degree at Universitat Politècnica de Catalunya with "Excellent Cum Laude" in 2020. She currently works at the GNSS Research Center, Wuhan University, where her research focuses on ionospheric determination using GNSS data.

Qile Zhao received his doctoral degree from Wuhan University in 2004, and is currently a professor at the GNSS research center of Wuhan University. His current research interests are precise orbit determination and high-precision positioning with GPS, GLONASS, BeiDou, and Galileo.